Hopping conduction in a two-dimensional impurity band

G. Timp, A. B. Fowler, and A. Hartstein
IBM Thomas J. Watson Research Center, P.O. Box 218, Yorktown Heights, New York 10598

P. N. Butcher
University of Warwick, Coventry CV4 7AL, England, United Kingdom
(Received 18 April 1985; revised manuscript received 21 April 1986)

The temperature dependence (380 mK $< T <$ 80 K) and electric field dependence (50 mV/cm $< F <$ 150 V/cm) of hopping conduction have been measured as a function of the impurity concentration, surface electric field, and carrier density in a quasi-two-dimensional impurity band formed in the inversion layer of a sodium-doped silicon metal-oxide—semiconductor field-effect transistor. The conductivity is found to be an exponential function of the temperature and applied electric field. Our observations can be accommodated by noninteracting, single-particle hopping models based on percolation theory in which the Coulomb repulsion between electrons on different sites is ignored. For impurity concentrations in the range 2×10^{11} to 1.14×10^{12} cm^{-2} and localization lengths from 3.4 to 7.5 nm, the noninteracting theories accurately describe eight-orders-of-magnitude change in the conductivity of a half-filled impurity band observed for a factor-of-80 change in temperature, and three-orders-of-magnitude change in the non-Ohmic current observed for a factor-of-15 change in electric field. The observed temperature dependence of the conductivity is not consistent with the temperature dependence predicted by Efros and Shklovskii for a Coulomb gap in the single-particle excitation spectrum, although their theory was expected to predict the conductivity under the conditions examined in this experiment.

I. INTRODUCTION

A quasi-two-dimensional (2D) impurity band is formed in the inversion layer of sodium-doped silicon metal-oxide—semiconductor field-effect transistor (MOSFET) by drifting sodium ions from the gate electrode through the silicon dioxide to the silicon-silicon dioxide interface.[1,2] Electrons in the inversion layer are bound by the Coulomb potentials of sodium ions randomly distributed throughout the oxide near the interface. The site energies are distributed over a finite bandwidth either because of random potential fluctuations associated with the interface or because of the random positions of the impurities in the oxide. If the oxide near the Si-SiO_2 interface is lightly doped with sodium so that the average distance between impurities is sufficiently greater than the effective Bohr radius of the bound states, then the electronic system in the inversion layer is strongly localized.[3] The conductivity in a lightly doped impurity band vanishes as the temperature approaches zero. At finite temperatures two conduction mechanisms occur in parallel: hopping and the thermal excitation of carriers from the impurity band to extended states above the mobility edge.

When the number of electrons is less than one per site, and the thermal energy is less than the binding energy, the conductivity is dominated by hopping or thermally assisted tunneling between localized states in the band. Hopping occurs because of the exponentially small overlap between the bound states on different sites. The difference between the initial and final site energies corresponding to a single hop is conserved by thermal fluctuations in the lattice. Two models based on classical percolation theory have been proposed to describe hopping conduction in a 2D impurity band. Hayden and Butcher[4] have developed a model in which the electrical conductivity is determined by single-particle hops from singly occupied to vacant sites in a uniform density of localized states distributed over a finite bandwidth, while the Coulomb repulsion between electrons on different sites is ignored. Efros and Shklovskii,[5] and Pollak[6] have argued, on the contrary, that the intersite Coulomb repulsion cannot be neglected and that the effect of electron-electron interactions is to reduce the number of low-energy one-particle hops so that the conductivity in a 2D impurity band is determined by excitations across a (Coulomb) gap in the single-particle density of states. The sodium-doped MOSFET represents a unique opportunity for the evaluation of models for hopping conduction because, in addition to changing the temperature and electric field, relevant parameters such as the localization length, the density of states, and the carrier density can be varied by changing the substrate bias, the sodium concentration, and the gate voltage, respectively.[1,2] However, the application of specific models for 2D hopping conduction has been problematic because of the limited scope of systematic experimental results.

We report the results of a comprehensive evaluation of noninteracting, single-particle models for hopping conduction between strongly localized states in a quasi-2D impurity band in this paper. We have measured the temperature dependence and electric field dependence of hopping conduction in an impurity band formed in the inversion layer of a sodium-doped Si MOSFET at a series of sodium concentrations, surface electric fields, and gate voltages, and compared the results with noninteracting, single-particle hopping models in which the intersite Coulomb repulsion between electrons is ignored. The con-

 ©1986 The American Physical Society

ductivity is found to be an exponential function of both the temperature and applied electric field. Our observations can be accommodated by the noninteracting models for Ohmic conduction due to Hayden and Butcher[4] and for non-Ohmic conduction due to Shklovskii.[7] The observed temperature dependence of the conductivity is not consistent with the temperature dependence predicted by Efros and Shklovskii[5] for a Coulomb gap in the single-particle excitation spectrum, although their theory was expected to predict the conductivity under the conditions examined in this experiment.

Previous work has also been shown to be consistent with the noninteracting theory but the interpretation was equivocal. Mott *et al.*[8] demonstrated that the temperature dependence of the Ohmic conductivity of an inversion layer associated with localized states in the conduction-band tail is consistent with the law $\sigma=\sigma_0\exp[-(T_0/T)^{1/3}]$ over the range (600 mK $< T <$ 2.9 K), but did not quantitatively investigate the dependence of the parameter T_0 on the density of states or the exponential decay rate of the localized state which are parameters of the theory or report non-Ohmic conduction for weak electric fields which is characteristic of hopping. In addition, Mott could not unambiguously examine the temperature dependence of the hopping conduction in the band tail for $T > 3$ K because the conductivity is dominated by activation to the mobility edge. Fowler and Hartstein[1,2] investigated the dependence of the high-temperature ($10 < T < 40$ K) activated Ohmic conductivity in a 2D sodium impurity band on substrate bias, sodium concentration, and carrier density, but did not examine the temperature dependence over the entire range where the noninteracting model applies nor report non-Ohmic conduction for weak electric fields. In comparison, we have investigated the temperature dependence (380 mK $< T <$ 40 K) of the Ohmic conductivity, the electric field dependence (50 mV/cm $< F <$ 150 V/cm) of the non-Ohmic conductivity, and the dependence of the Ohmic conductivity on the localization length and the density of localized states over the entire range where the noninteracting models apply, while our results for the Ohmic conductivity obtained in the high-temperature and low-temperature limits are consistent with earlier work.

This paper is organized into five sections. Section II is devoted to the details of the experiment and a discussion of the experimental results. In Sec. III we examine the salient features of the noninteracting models for Ohmic hopping conduction due to Hayden and Butcher[4] and for non-Ohmic conduction due to Shklovskii[7] which are used in the interpretation of the data. In Sec. IV the predictions of the theory are compared with the experimental data, and trends observed in the exponential decay rate of the localized state and in the density of states as a function of substrate bias, impurity concentration, and carrier density are discussed. Finally, in Sec. V we summarize the main results.

II. EXPERIMENTAL RESULTS

We have made two point drain-source conductance measurements on five n-channel circular gate sodium-doped MOSFET's as a function of temperature and electric field. The circular gate MOSFET devices used in these experiments were fabricated on (100) silicon surfaces, and have a channel length of 10 μm and a gate oxide thickness of 100 nm. The bulk resistivity of the silicon was 2 Ω cm. The gate oxide was purposefully contaminated with approximately 2×10^{13} cm^{-2} of NaCl prior to the gate metallization step in the fabrication so that during the experiment the Na^+ concentration near the interface could be changed. The Na^+ surface concentration, N_{ox}, in each sample was varied by applying positive gate voltages ($\sim$10 V) to drift sodium ions from the gate electrode to the Si-SiO_2 interface at room temperature. The resulting sodium impurity distribution in the oxide is within 5 nm of the interface.[9] The surface concentration was determined from the threshold voltage observed in the transconductance at a temperature of 77 K. It has been shown[2] that a discrepancy exists between this value and the impurity concentration deduced from Shubnikov–de Haas measurements. Although the relative change in N_{ox} can be determined to within 10%, the estimate of the absolute concentration deduced from the transconductance may be in error by as much as 1×10^{11} cm^{-2}.

For electric fields $F < 100$ mV/cm peak to peak the electrical conductivity of the inversion layer was Ohmic for the range of temperature, impurity concentration, substrate bias, and carrier density examined in these experiments. The temperature dependence of the Ohmic conductivity was investigated using a lock-in technique at frequencies ranging from 0.20 to 150 Hz. The Ohmic conductivity was not frequency dependent in the accessible temperataure range. At temperatures $T < 40$ K, a maximum was observed in the Ohmic electrical conductivity as a function of carrier density, n, below threshold. The Ohmic conductivity of the inversion layer as a function of the change in carrier density δn is shown in Figs. 1(a), (b), and (c) for a series of sodium concentrations, substrate bias conditions, and temperatures, respectively. The maximum observed in the conductance has been interpreted as evidence of a band in the density of localized states lying ($\sim$20 meV) below the lowest electric subband in the silicon.[1,2] We assume that the peak in the conductivity corresponds to a half-filled nondegenerate sodium impurity band, i.e., one half electron per sodium site. A maximum in the conductance has been reported only in sodium-doped MOSFET's and was not observed in this work for N_{ox} below 1.5×10^{11} cm^{-2} at $T > 30$ K with an excitation of 500 μV and a current sensitivity of 100 fA. As shown in Fig. 1, the half width at half maximum of the peak as a function of carrier density is independent of substrate bias and temperature but increases with sodium concentration, while the magnitude of the peak conductivity increases dramatically as the sodium concentration and temperature increase, and as the substrate bias becomes more positive. We note that the energy bandwidth is not simply related to the change in carrier density since $\delta n=\int_E^{E+\delta E}\rho(E)dE$, where ρ is the density of states in the impurity band, and ΔE is the change in the Fermi energy. Consequently, the width of the peaks in the conductance as a function of carrier density shown in Fig. 1 are not indicative of the

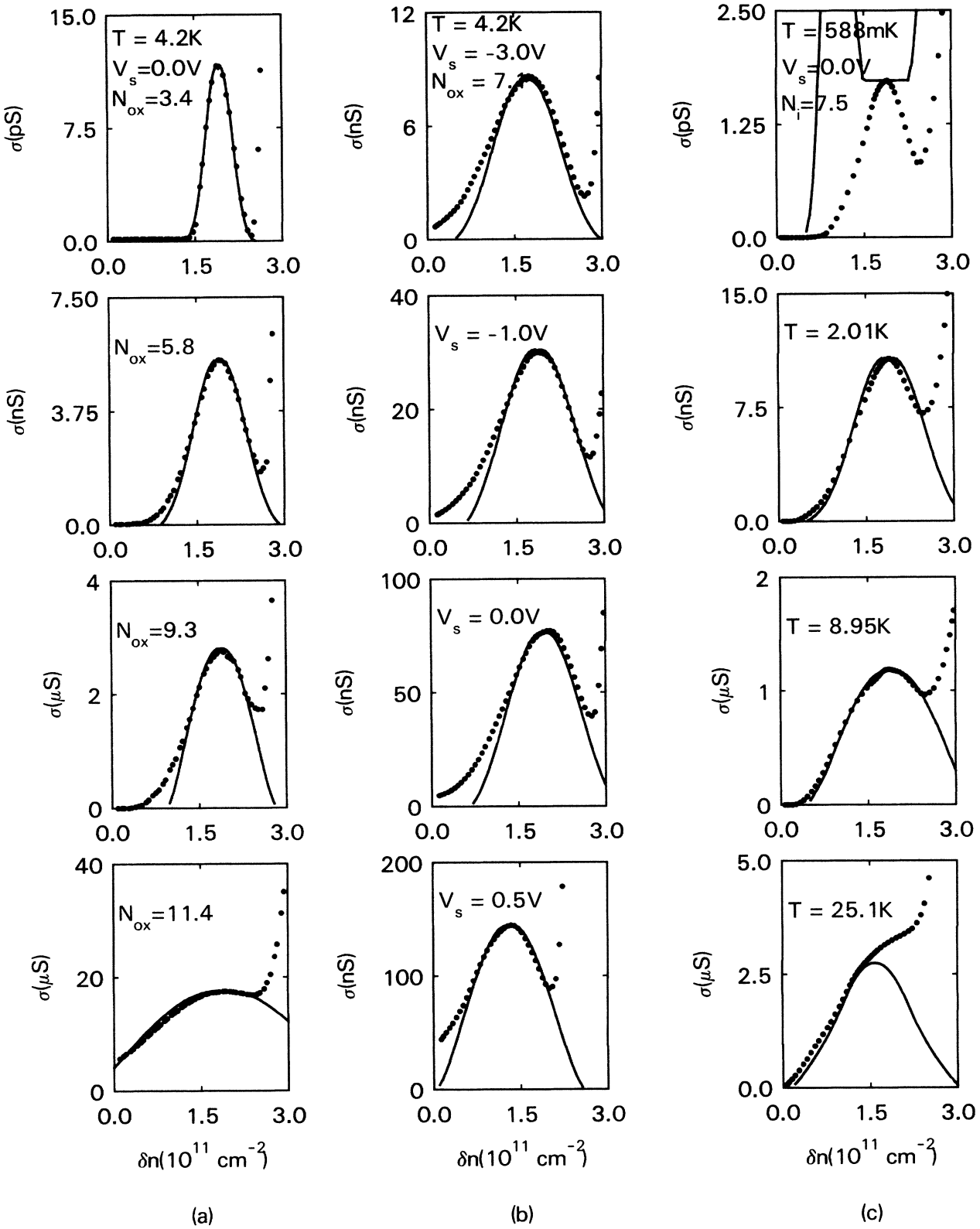

FIG. 1. Typical plots of the MOSFET channel conductivity σ vs the change in carrier density, δn, below threshold in the Ohmic regime. From top to bottom: (a) shows the conductivity vs δn at $T=4.2$ K, $V_s=0.00$ V for impurity concentrations of $N_{ox}=3.4$, 5.8, 9.3, and 11.4×10^{11} cm^{-2}; (b) shows the conductivity vs δn for a substrate bias of $V_s=-3.0$, -1.0, 0.0, and 0.5 V at $T=4.2$ K and $N_{ox}=7.1\times10^{11}$ cm^{-2} and; (c) shows the conductivity vs δn at $V_s=0$ V and $N_{ox}=7.5\times10^{11}$ cm^{-2} at temperatures of 588 mK, 2.01, 8.95, and 25.1 K. The dots represent experimental values while the solid lines in the figure represent the fit of the model to the data. The discrepancy between the data and the model for $f\neq0.5$ in the top of Fig. 1(c) is not shown entirely. The calculated result peaks at $\sigma=4$ pS, $\delta n=1.0$, 2.75×10^{11} cm^{-2}.

bandwidth.

For a particular substrate bias and sodium concentration, the temperature dependence of the channel current was studied as a function of carrier density by sweeping the voltage on the gate electrode at fixed temperatures. The conductivity was measured at approximately 300 different temperatures ranging from 380 mK to 80 K for each gate voltage. The temperature was determined from a germanium resistance thermometer in thermal contact with a copper block which held the sample header. The copper block and the device under study were mounted on a shielded sample holder. The device was either immersed in liquid ^{4}He or an exchange gas in a conventional cryostat to obtain temperatures in the range 1.30 to 80 K, or immersed in liquid ^{3}He in an evaporation cryostate used in conjuction with the conventional cryostate to obtain temperatures as low as 360 mK. For $T > 1.3$ K the temperature was regulated by a computer-controlled current source which monitored the germanium thermometer and adjusted the heater current to maintain temperature stability. For temperatures 360 mK $< T < 2.9$ K the tempera-

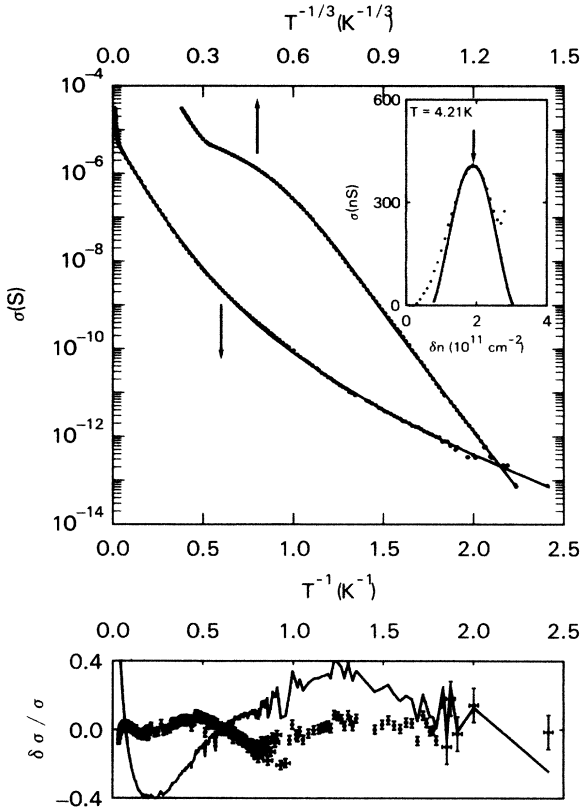

FIG. 2. Temperature dependence of the Ohmic conductivity of a half-filled band for $N_{ox}=8.1\times10^{11}$ cm^{-2} and $V_s=0$ V. In the figure the logarithm of the conductivity is plotted against both T^{-1} and $T^{-1/3}$. The solid lines in the figure represent a fit of the HB model to the data over the temperature range 400 mK $< T <$ 30 K using the parameters $g_0=53.3$ mS, $\alpha^{-1}=5.26$ nm, $W=3.75$ meV, and $N_i=2.93\times10^{11}$ cm^{-2}. The inset in the upper right corner shows the dependence of the conductivity on gate voltage observed at 4.2 K. The arrow indicates the gate voltage corresponding to a half-filled band. In the lower portion of the figure the deviation of the fit from representative data points (the dots with error bars) is plotted against reciprocal temperature. The line in the lower portion of the figure represents the deviation of a fit to a $T^{-1/2}$ law over a temperature range in which the optimum exponent is one-half.

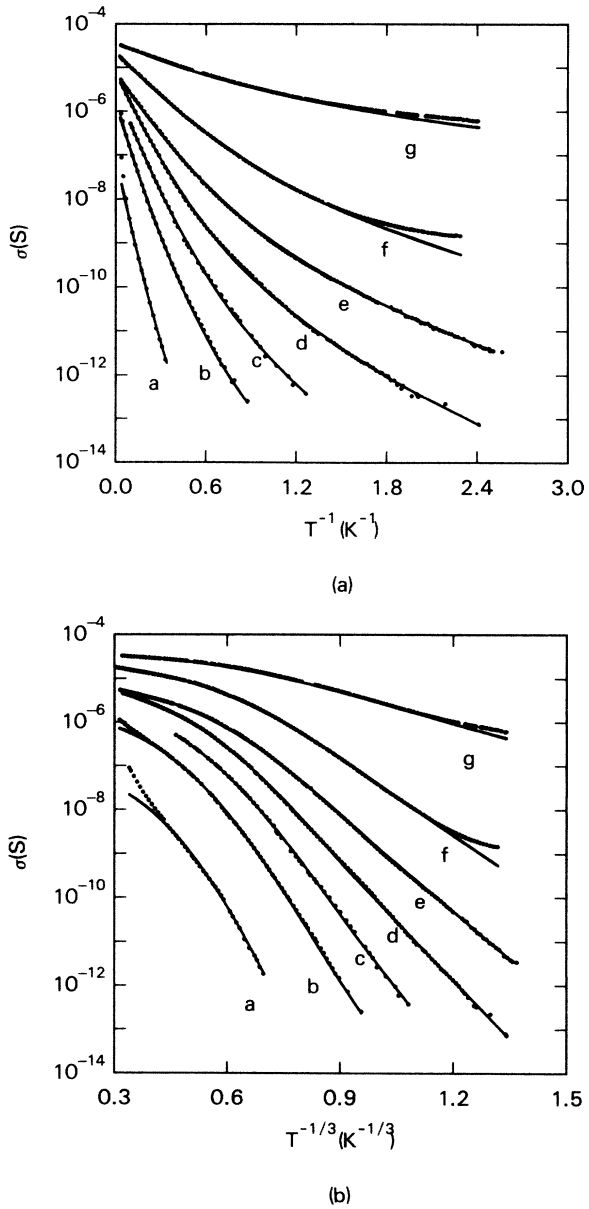

FIG. 3. Temperature dependence of the Ohmic conductivity of a half-filled band as a function of impurity concentration at $V_s=0.00$ V. In (a) the Ohmic conductivity is plotted vs T^{-1}. In (b) the same data as (a) are shown vs $T^{-1/3}$. The parameters used for the fits to the data (indicated by the solid line in the figure) are a, $W=8.36$ meV, $\alpha^{-1}=4.56$ nm, $g_0=527$ mS; b, $W=5.92$ meV, $\alpha^{-1}=4.41$ nm, $g_0=435$ mS; c, $W=4.53$ meV, $\alpha^{-1}=4.54$ nm, $g_0=285$ mS; d, $W=3.74$ meV, $\alpha^{-1}=4.49$ nm, $g_0=252$ mS; e, $W=3.75$ meV, $\alpha^{-1}=5.85$ nm, $g_0=53.3$ mS; f, $W=2.61$ meV, $\alpha^{-1}=5.56$ nm, $g_0=28.3$ mS; g, $W=1.79$ meV, $\alpha^{-1}=5.97$ nm, $g_0=4.75$ mS corresponding to impurity concentrations of a, 3.4, b, 5.7, c, 6.6, d, 7.5, e, 8.1, f, 9.38, and g, 11.4×10^{11} cm^{-2} with $N_i=N_{ox}/(2.75\pm0.35)$.

ture was controlled using a manostate to regulate the vapor pressure over liquid ^{3}He or ^{4}He. The temperature range of the data was ultimately determined by a 20-fA noise level associated with the current-sensitive preamplifier and the lock-in–amplifier detection equipment.

Figure 2 shows the temperature dependence of the conductivity typically observed for a half-filled band over the temperature range 400 mK to 80 K. The same data are plotted against both $T^{-1/3}$ and T^{-1}. At high temperature ($40 < T < 80$ K) the transport is approximately activated corresponding to thermal excitation to the mobility edge.[1] At low temperature (400 mK $< T <$ 30K) the conductivity is determined by hopping. As shown in Fig.

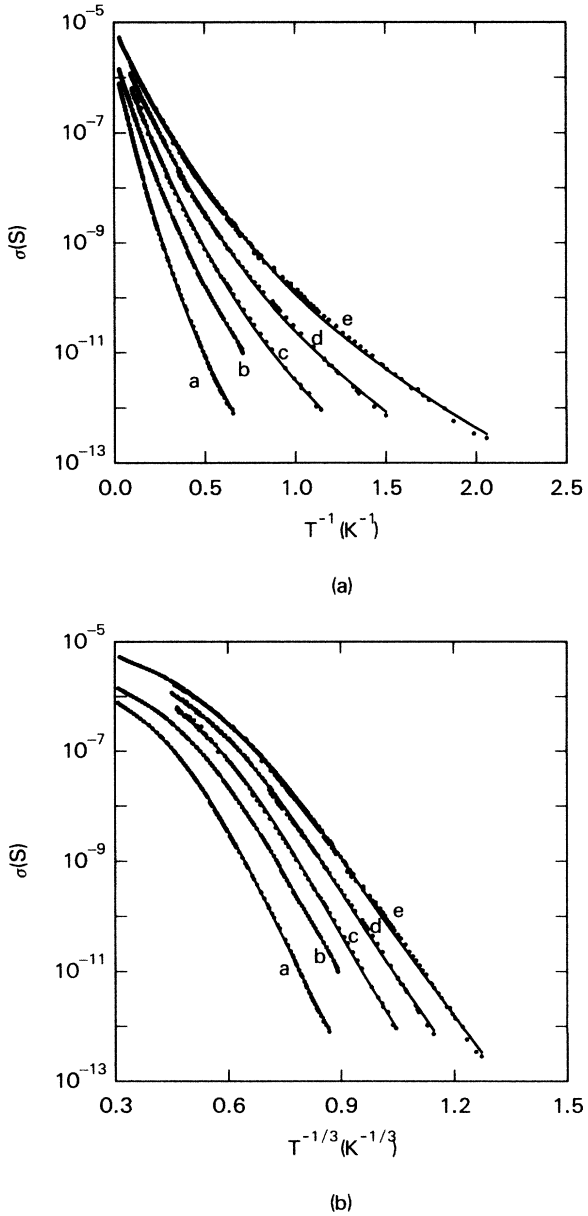

FIG. 4. Temperature dependence of the Ohmic conductivity as a function of substrate bias at $N_{ox}=7.5\times10^{11}$ cm^{-2} with ($N_i=2.8\times10^{11}$ cm^{-2}). In (a) the temperature dependence is shown vs T^{-1}. In (b) the same data as (a) is plotted vs $T^{-1/3}$. The parameters used for the fits to the data (indicated by the solid line in the figure) are a, $W=7.38$ meV, $\alpha^{-1}=4.11$ nm, $g_0=301$ mS; b, $W=5.49$ meV, $\alpha^{-1}=4.49$ nm, $g_0=157$ mS; c, $W=4.36$ meV, $\alpha^{-1}=4.15$ nm, $g_0=454$ mS; d, $W=3.74$ meV, $\alpha^{-1}=4.56$ nm, $g_0=252$ mS; e, $W=3.21$ meV, $\alpha^{-1}=4.73$ nm, $g_0=150$ mS; for a substrate bias of a, 8.0 V; b, -3.0 V; c, -1.0 V; d, 0.0 V; and e, 0.50 V, respectively.

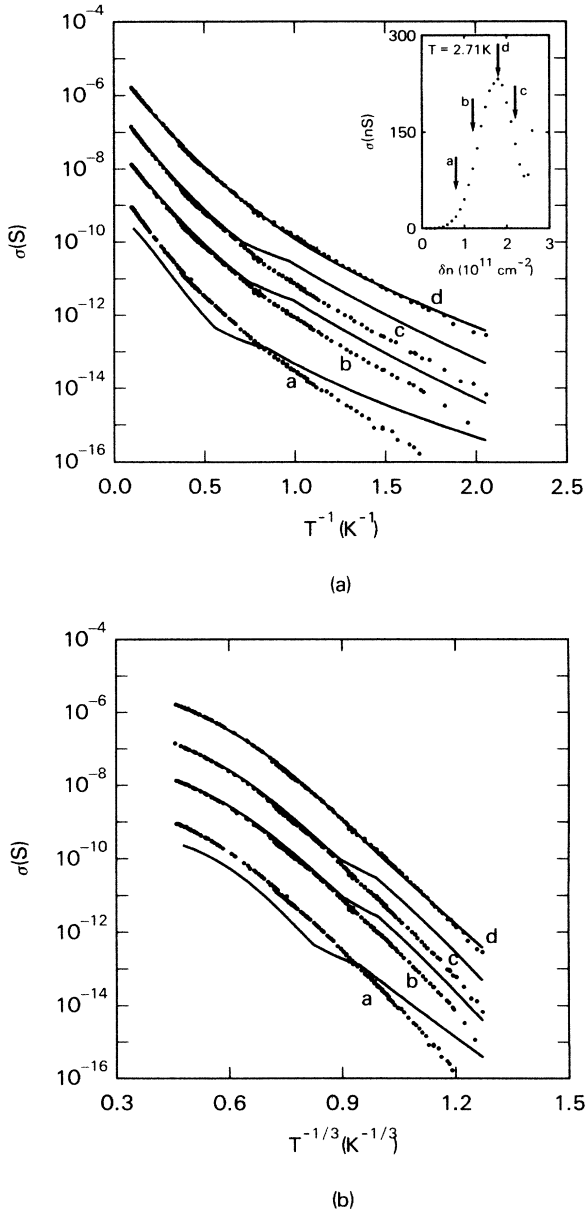

FIG. 5. Temperature dependence of the Ohmic conductivity as a function of the filling fraction observed at $V_s=0.50$ V for $N_{ox}=7.5\times10^{11}$ cm^{-2} ($N_i=2.8\times10^{11}$ cm^{-2}). For clarity, the conductivity data of curves a, b, and c were divided by 1000, 100, and 10, respectively. In (a) the temperature dependence is plotted vs T^{-1}. In (b) the same data as (a) is shown on a $T^{-1/3}$ scale. The parameters used for the fits to the data (indicated by the solid lines) are $g_0=150$ mS, $W=3.2$ meV, $\alpha^{-1}=4.73$ nm for the corresponding filling fractions of a, 0.09 b, 0.33, c, 0.69, and d, 0.50. The conductivity as a function of gate voltage is shown in the inset of (a). The gate voltages corresponding to the various filling fractions are indicated in the inset.

2, the activation energy corresponding to hopping conduction, determined from the slope of the logarithm of the conductivity as a function of reciprocal temperature, decreases with temperature. At temperatures $T<4.0$ K, the logarithm of the conductivity follows a $T^{-1/3}$ law. Figures 3, 4, and 5 show the temperature dependence of the conductivity of a half-filled band in the hopping regime (370 mK $< T <$ 30 K) for seven different impurity concentrations at one substrate bias, five different substrate bias conditions at one concentration, and four different filling fractions at one substrate bias and impurity concentration, respectively. As shown in Figs. 3(a), 4(a), and 5(a), with increasing substrate bias, increasing sodium concentration, and either an increase or decrease in filling fraction toward one-half, the high-temperature slope versus reciprocal temperature decreases and the curvature increases. In Figs. 3(b), 4(b), and 5(b) the data of Figs. 3(a), 4(a), and 5(a) are replotted as a function of $T^{-1/3}$. We observe that the low-temperature slope on a $T^{-1/3}$ scale decreases with increasing substrate bias and increasing impurity concentration. As a function of carrier density we find that the deviations from a $T^{-1/3}$ law to a dependence T^{-x} with $x>\frac{1}{3}$ are pronounced at low temperature. The data shown in Figs. 2, 3, 4, and 5 are representative of the results obtained on three different samples, five different sodium concentrations per sample, four different substrate bias conditions per sodium concentration, and ten different gate voltage per substrate bias.

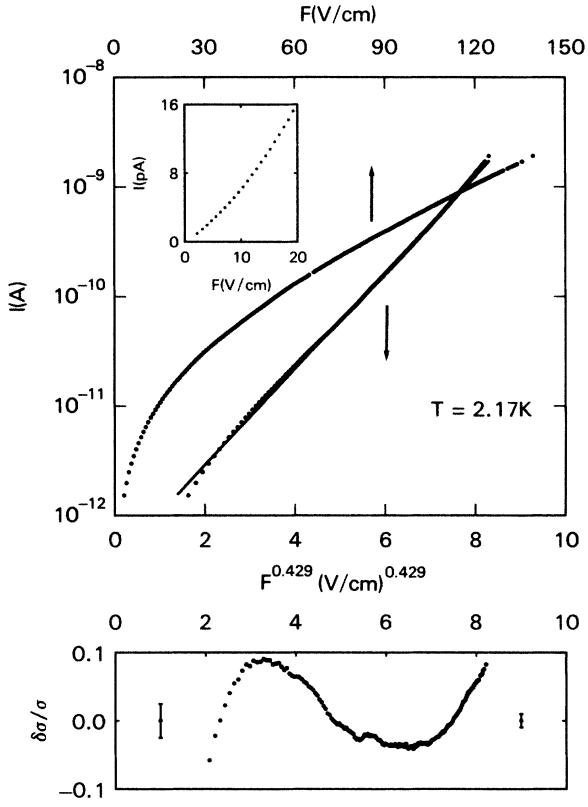

FIG. 6. Electric field dependence of the non-Ohmic hopping current at 2.17 K for a half-filled impurity band, $V_s=0$ V and $N_{ox}=5.6\times10^{11}$ cm^{-2} ($N_i=2.8\times10^{11}$ cm^{-2}). The same data are plotted against a, F and b, $F^{0.429}$. The solid line in the figure represents the fit to the data using Shklovskii's theory for non-Ohmic conduction applied to two dimensions. The fitting parameters $F_0=1.03$ mV/cm. The inset in the upper left corner shows the deviation from Ohmic behavior observed at low fields. In the lower portion of the figure the deviation of the fit from the data is represented and a typical error is indicated.

For electric fields $2<F<150$ V/cm, we observed non-Ohmic conduction. We assume that the nonlinearity is due to the hopping mechanism since the Fermi energy and the thermal energy are both much less than the binding energy. The current-electric field characteristic of the inversion layer was measured at dc using an electrometer. For each substrate bias and impurity concentration the dependence of the channel current on the drain-source voltage was examined for a half-filled band at approximately 200 different fields uniformly distributed from 0 to 150 V/cm as a function of temperature, impurity concentration, and substrate bias. Over this field range, the current was independent of the polarity of the electric field with respect to a grounded source contract, while for $F>200$ V/cm the channel current depended on the voltage polarity. A voltage drop between the drain and source contacts changes the position of the Fermi level in the density of localized states across the channel length. For $F<150$ V/cm the change in the density of states at the Fermi level is negligible because the current is independent of polarity, but for $F>200$ V/cm the change in the density of states is significant. Figure 6 shows a typical plot of the logarithm of the channel current versus electric field F at a temperature of 2.17 K. The same data are plotted versus both F and $F^{0.429}$ in the figure. We observe that the non-Ohmic current is an exponential function of $F^{0.45\pm0.07}$ for $5<F<130$ V/cm. This plot is representative of data obtained on two samples for four sodium concentrations, four substrate bias conditions per sodium concentration, and four temperatures per substrate bias.

III. THEORETICAL MODELS FOR HOPPING CONDUCTION

To interpret the Ohmic conductivity data, we adopted a model developed by Hayden and Butcher[4] (HB) for hopping conduction in a 2D impurity band in which the density of states ρ, and the coefficient of exponential decay of the localized state α are assumed to be constant over a bandwidth W below the mobility edge E_c, i.e., the probability that a given site has an energy ε_i is assumed to be independent of the other site energies and of the site number, and was taken to be

$$\rho(\varepsilon_i)=\begin{cases}N_i/W, & |\varepsilon_i|\le W/2\\ 0, & |\varepsilon_i|>W/2\end{cases} \tag{1}$$

where N_i denotes the site density [$\int\rho(E)dE=N_i\le N_{ox}$]. States which are above E_c, corresponding to the lowest electric subband in the silicon inversion layer, are assumed

to be extended. In the model, the structure of the bound-state wave function is assumed to be the same as for an isolated impurity and the overlap between sites is assumed to depend exponentially on the intersite separation r_{ij}, while the intersite Coulomb repulsion between electrons is ignored and the intrasite Coulomb interaction is assumed to be large compared to the binding energy so that the occupied states are nondegenerate. The chemical potential at $T=0$ is assumed to be in the impurity band.

Extending the ideas of Ambegaokar, Halperin, and Langer,[10] Hayden and Butcher[4] assert that the calculation of the dc hopping conductivity in a 2D impurity band of finite width reduces to the problem of calculating the conductivity of an equivalent Miller-Abrahams[11] (MA) conductance network where the conductances represent the transition rates for noninteracting single-electron hops between sites. The approximation that is adopted for the conductance between two sites (i,j) is

$$G_{ij}=\sigma_0\exp\left[-2\alpha r_{ij}-\frac{|\tilde{\varepsilon}_i|+|\tilde{\varepsilon}_j|+|\tilde{\varepsilon}_i-\tilde{\varepsilon}_j|}{2kT}\right]$$
$$=\sigma_0 e^{-\xi_{ij}} \tag{2}$$

so that the hopping current between sites i and j is written

$$J_{ij}=G_{ij}\frac{kT}{e}\left[\exp\left[\frac{\delta\mu_i-\delta\mu_j}{kT}\right]-\exp\left[\frac{e\mathbf{F}\cdot\mathbf{r}_{ij}}{kT}\right]\right], \tag{3}$$

where $\mathbf{r}_{ij}$ is the intersite distance vector, the initial- and final-state site energies are, respectively, $\tilde{\varepsilon}_i=\varepsilon_i-\tilde{\mu}$ and $\tilde{\varepsilon}_j=\varepsilon_j-\tilde{\mu}$, with $\tilde{\mu}=\mu+kT\ln(g)$. The chemical potential μ is measured relative to the center of the band and g, the band degeneracy factor, is equal to 4 in a (100) inversion layer because of the two-fold spin degeneracy and the two-fold valley degeneracy, the change in the chemical potential due to the electric field is represented by $\delta\mu_i$, and k is the Boltzmann constant. The exponential functions in Eq. (3) can be linearized for sufficiently weak electric fields so that Eq. (3) becomes

$$J_{ij}=\frac{G_{ij}}{e}(\delta\mu_i-\delta\mu_j-e\mathbf{F}\cdot\mathbf{r}_{ij}) . \tag{4}$$

A justification for this approximation to the current is given elsewhere.[4]

Formula (4) is the basis of the MA resistor network. The nodes of the network are at electrochemical potentials of $\delta\mu_i-e\mathbf{F}\cdot\mathbf{r}_{ij}$ and are interconnected by the conductances G_{ij}. Since the exponent in the conductivity ξ_{ij} is the sum of random variables, the individual resistances have an exponential scatter. Because the values of the individual resistances are stochastic and vary over many orders of magnitude, the overall electrical conductivity of the network is determined by the critical percolation conductance, $G_c=\sigma_0\exp(-\xi_c)$, defined as the largest value of the conductance such that the subset of resistors with $G_{ij}>G_c$ still contains a connected network which spans the entire system. The salient feature of the percolation model for the conductivity is the critical resistance subnetwork composed of a limited number of critical percolation conductances linked by low-resistance paths which represent hops with exponentially larger transition probability. Resistors with $G_{ij}\ll G_c$, corresponding to hops with an exponentially smaller transition probability, are effectively shorted out. Since in the main only resistors with $\xi_{ij}<\xi_c$ contribute to the conduction, if we determine the critical resistance and calculate the conductivity of the network assuming that the network is composed only of conductances larger than G_c, then we can obtain a lower bound to the conductance of the network.

To determine the critical percolation conductance, it is assumed after Seager and Pike[12] that the number of conductances per site which link the individual sites to the network, N_c, is invariant at the percolation threshold, depending only on the dimensionality and topology of the system. For a two-dimensional system,[12,13] in which the site energy is treated as an additional degree of freedom, $N_c=2.7$. However, at high temperature, where the degree of freedom associated with the site energy can be ignored, $N_c=4.5$. To accommodate the change in N_c we assume after Hayden and Butcher that $N_c=2.7$ for $T<T'$ and

$$N_c=2.7+(4.5-2.7)(1-T'/T)$$

for $T>T'$, where

$$T'=(\pi N_i W^3/128 N_c\alpha^2 k)^{1/2} .$$

The value of the critical conductance is deduced by calculating the number of conductances per site and requiring that the number be equal to N_c. The average number of conductances per site with $\xi_{ij}<\xi_c$ is given by

$$\langle N\rangle=\frac{\int\rho(\tilde{\varepsilon}_i)d\tilde{\varepsilon}_i\int\rho(\tilde{\varepsilon}_j)d\tilde{\varepsilon}_j\int 2\pi r\,dr}{\int\rho(\tilde{\varepsilon}_i)d\tilde{\varepsilon}_i} , \tag{5}$$

where ρ represents the density of states and limits on the integrals are evaluated according to the criterion $\xi_{ij}<\xi_c$. The condition that $N_c=\langle N\rangle$ determines the exponent ξ_c, and the critical conductance G_c.

According to the HB model, the conductivity of the network can be generally expressed as a configurational average over all conductances such that $\xi_{ij}\neq\xi_c$. The result of the configurational average is

$$\sigma=g_0\sigma_c e^{-\xi_c} . \tag{6}$$

The prefactor σ_c in Eq. (6) represents the contribution of the other resistors ($G_{ij}\neq G_c$) in the MA network to the conductivity. The factor g_0 is a measure of the electron-phonon interaction and is proportional to the hopping rate. The parameter g_0 is assumed to be a constant independent of temperature in our subsequent analysis. As a function of temperature the conductance σ for a 2D impurity band is obtained by solving[4]

$$N_c=\frac{\pi}{24}\left[\frac{N_i kT}{\alpha^2 W}\right]\times\begin{cases}\frac{3}{2}\xi_c^3, & \xi_c<K'\\ \dfrac{3\xi_c^4-2(\xi_c-K')^3(\xi_c+K')}{\xi_c+K'}, & K'<\xi_c<J'\\ \dfrac{3\xi_c^4-2(\xi_c-K')^3(\xi_c+K')-2(\xi_c-J')^3(\xi_c+J')}{J'+K'}, & J'<\xi_c<2W'\\ \dfrac{3\xi_c^2-2(\xi_c-K')^3(\xi_c+K')-2(\xi_c-J')^3(\xi_c+J')+(\xi_c-J'-K')^4}{J'+K'}, & 2W'<\xi_c\\ \dfrac{(\xi_c+K')^4-5(\xi_c-J')^4-(\xi_c-J')^3(\xi_c+3J'+4K')}{J'+K'}, & K'<0 \text{ and } J'<\xi_c\end{cases} \tag{7a}$$

for ξ_c. The evaluation of the prefactor σ_c in Eq. (6) follows from

$$\sigma_c=\frac{\pi}{160}\left[\frac{N_i kT}{\alpha^2 W}\right]^2\times\begin{cases}3\xi_c^5, & \xi_c<K'\\ 3\xi_c^5-(3K'+2\xi_c)(\xi_c-K')^4, & K'<\xi_c<J'\\ 3\xi_c^5-(3K'+2\xi_c)(\xi_c-K')^4-(3J'+2\xi_c)(\xi_c-J')^4, & J'<\xi_c<2W'\\ 3\xi_c^5-(3K'+2\xi_c)(\xi_c-K')^4-(3J'+2\xi_c)(\xi_c-J')^4+(\xi_c-J'-K')^5, & 2W'<\xi_c\\ (\xi_c+K')^5-5(\xi_c+K')(\xi_c-J')^4+4(\xi_c-J')^5, & K'<0 \text{ and } J'<\xi_c\end{cases} \tag{7b}$$

once ξ_c has been determined. In Eqs. (7) $K'=W'+\mu', J'=W'-\mu'$, where $W'=W/2kT$ and $\mu'=\tilde{\mu}/kT$. If we assume that the site energies are distributed below the mobility edge according to Eq. (1), then the temperature dependence of the chemical potential is determined from the condition

$$f=\frac{n}{N_i}=\frac{1}{W}\int_{-W/2}^{W/2}d\varepsilon\frac{1}{1+e^{(\varepsilon-\tilde{\mu})/kT}}+\frac{\rho_s}{N_i}\int_{E_c}^{\infty}d\varepsilon\frac{1}{1+e^{(\varepsilon-\mu)/kT}} \tag{8}$$

assuming that the carrier density n is constant. The parameter $\rho_s=1.6\times10^{11}\ \mathrm{cm}^{-2}\mathrm{meV}^{-1}$ represents the density of states associated with the fourfold-degenerate lowest electric subband in the silicon inversion layer. In Eq. (8) we have assumed that the degeneracy of the conduction band is not effected by its occupation and so consequently, only the chemical potential appears in the second term on the right-hand side of Eq. (8).

A thorough interpretation of Eq. (7) was given in Ref. 4; the only difference between these results and those reported by Hayden and Butcher, apart from typographical errors in Ref. 4, is that here the effect of a temperature-dependent chemical potential has been included. The temperature dependence of the chemical potential of a half-filled band [$f=0.5$ in Eq. (8)] is dominated by $-kT\ln4$ for $16<E_c<30$ meV (Ref. 15) and temperatures below 40 K, so that the quantity $\mu+kT\ln4$ which is important in the model for hopping conduction does not change appreciably as a function of temperature. Because the contribution of the second term on the right-hand side of Eq. (8) to the temperature dependence of the chemical potential for $T<30$ K is negligible, it will be ignored in our subsequent analysis. For temperatures $T>40$ K the chemical potential becomes more negative with increasing temperature relative to the center of the band because the carrier concentration in the lowest subband in the silicon increases. The chemical potential, μ, may change by 10 meV for $1<T<80$ K.

For a half-filled impurity band ($f=0.5$, $\tilde{\mu}=0$) the model represented by Eq. (7) has three adjustable parameters: $\alpha N_i^{-1/2}$, W', and g_0. As expected, for $\xi_c<W'$ the Ohmic conductivity has the form

$$\sigma\sim(T_0/T)\exp[-(T_0/T)^{1/3}],$$

where $kT_0=13.75\alpha^2/\rho$, corresponding to the Mott[8] result in two dimensions, while for $2W'\le\xi_c$ the expression for ξ_c reduces to

$$\xi_c=\frac{5W}{12kT}+\left[\frac{4N_c\alpha^2}{\pi N_i}\right]^{1/2}\times\left[1-\frac{5\pi}{576N_c}\left[\frac{W}{kT}\right]^2\frac{N_i}{\alpha^2}\right]^{1/2}, \tag{9}$$

so that the transport is approximately activated with an activation energy of $5W/12$. As a consequence of the finite band width, both a $\sigma\sim\exp[-(T_0/T)^{1/3}$ law and activated transport are expected to be observed in the conductivity in a temperature range $T<W/k\xi_c$. For $f\neq0.5$ there is an additional parameter, the filling fraction f, which enters through the chemical potential. An $\exp[-(T_0/T)^{-1/3}]$ law is predicted for $\xi_c<K'$ and at high temperature the conductivity is expected to be activated with an activation energy that increases from a minimum at $f=0.5$.

In the percolation model for hopping conduction, the conductivity of the network is dominated by a few key

conductances, $\sigma_0 \exp(-\xi_c)$, close to the percolation threshold, which are interconnected by resistances with $G_{ij} > G_c$. Because the hopping current is continuous, the drop in the electrochemical potential occurs inhomogeneously throughout the subnetwork across the critical percolation conductances while the transition rates corresponding to the these conductances are exponentially dependent on the electric field [see Eq. (3)]. Consequently, the onset of non-Ohmic behavior is expected for relatively weak electric fields.

To analyze the current-electric field characteristic of the inversion layer, we have adopted a model developed by Shklovskii[7] for non-Ohmic hopping conduction in thee dimensions. Shklovskii has shown that the current paths change in moderate electric fields and that the electric field has the effect of making the critical resistor subnetwork more homogeneous. Initially, as the electric field increases only the transition rate associated with the largest resistor in the critical subnetwork is nonlinear, but as the rate changes with electric field, the transition rate corresponding to the second largest resistor takes on equal importance, and consequently, the voltage is distributed between the two resistors. A further increase in the field results in a distribution of the voltage among an increasing number of resistors until ultimately the voltage is distributed homogeneously across the nonlinear resistors in the MA network. Shklovskii predicts that the field dependence of the current is given by

$$\ln\left[\frac{i}{\sigma(T)F_c}\right] = C\left[\frac{eFl}{kT}\right]^{1/(1+\nu)}, \qquad kT/el < F < kT\alpha/e \quad (10)$$

where the parameter ν is the critical index of the correlation length l (the average distance between the critical network nodes) in the percolation model,[13] $F_c = kT/el$, $\sigma(T)$ is given by Eq. (6), and $C \sim 1$ is a constant. The existence of a characteristic size of the critical network l, which is much larger than either the extent of the wave function or the average hopping length, is an essential feature of the theory. Note that the linearization in Eq. (4) is only possible if the criterion $F \ll F_c = kT/el$ is satisfied. In this limit Eq. (10) agrees with Eq. (6).

Shklovskii treats the three-dimensional case explicitly for temperatures in which the Ohmic conductivity satisfies $\sigma \sim \exp[-(T_0/T)^{1/4}]$ and assumes that $\nu \simeq 0.9$ and $l = \alpha^{-1}(T_0/T)^{(1-\nu)/4}$ appropriate to 3D, but since the description of the problem and the solution were formulated so that all the information on the topology of the system is included in the correlation length index ν, we assume that the result given in Eq. (10) can be applied to two-dimensions by taking $\nu \simeq 1.33$ and $l = \alpha^{-1}(T_0/T)^{(1+\nu)/3}$, which are appropriate to the two-dimensional case.[13] With these assumptions we find

$$\ln\left[\frac{i}{\sigma(T)F_c}\right] = C\left[\frac{eF}{\alpha kT}\right]^{1/(1+\nu)}\left[\frac{T_0}{T}\right]^{1/3}, \quad (11)$$

with $1/(1+\nu) = 0.429$ so that the slope of the logarithm of the non-Ohmic current versus $F^{0.429}$ is proportional to $(T_0/T)^{1/3}(\alpha kT)^{0.429}$.

IV. DISCUSSION

A. Ohmic conduction

We find that the Ohmic conductivity in a half-filled band is consistent with the noninteracting model for hopping conduction proposed by Hayden and Butcher (HB). To estimate the parameter $(\alpha N_i^{-1/2})$, the bandwidth W, and the hopping rate g_0, the data are fitted to the HB model over the temperature range $T < 30$ K. The range for which a particular condition (for example, $\xi_c < K'$) applies is determined self-consistently for a given choice of parameters. The data are fitted by solving Eq. (7) for each data point with an initial estimate of the parameters $(\alpha N_i^{-1/2})$, W, and g_0 [assuming $f = 0.5$ so that $\tilde{\mu}(T) = 0$] and then substituting the result for ξ_c and σ_c into Eq. (6). The choice of parameters is subsequently refined using a Davidson-Fletcher-Mitchell nonlinear fitting algorithm[14] to minimize the least-squares deviation of the fit from the data. A fit to the low-temperature hopping conductivity of a half-filled band using Eqs. (6) and (7), and varying the three parameters $\alpha N_i^{-1/2}$, W, and g_0, is represented by the solid line in Fig. 2. The optimum parameters for describing the data shown in Fig. 2 are $\alpha N_i^{-1/2} = 3.52$, $W = 3.75$ meV, and $g_0 = 53.3$ mS (1 S = 1 A/V). In the figure the logarithm of the conductance is plotted against both $T^{-1/3}$ and T^{-1} to emphasize the regime in which the conditions $\xi_c < K'$ and $2W' < \xi_c$ corresponding to variable-range hopping and activated transport are, respectively, satisfied. The temperatures corresponding to the conditions $\xi_c = K'$ and $2W' = \xi_c$ are 1.3 and 5.3 K, respectively. For the data shown, the entire range where the noninteracting hopping model applies (i.e., from $\xi_c < K'$ to $2W' < \xi_c$) must be used to fit the data. In the lower portion of Fig. 2 the relative deviation of the fit from the data, i.e., $\delta\sigma/\sigma = (\sigma_{\text{fit}} - \sigma_{\text{obs}})/\sigma_{\text{obs}}$, and the experimental error, are shown. The noninteracting HB model is consistent with the temperature dependence of the Ohmic conductivity observed over 8-orders-of-magnitude variation in the conductivity in the temperature range 400 mK $< T <$ 30 K. For $T > 30$ K the fit derived from the HB model deviates from the data because the conductivity is dominated by activation to the mobility edge.

The site density N_i can be deduced by fitting the conductivity as a function of carrier density at a fixed temperature assuming that g_0 is independent of n. According to the HB model, α and W are independent of n so that the conductivity as a function of carrier density depends only on the filling fraction $f = n/N_i$. Consequently, N_i can be determined from a one-parameter fit to the conductivity data as a function of carrier density. A typical fit to the data with $N_i = 2.93 \times 10^{11}$ cm^{-2} is shown in the inset of Fig. 2. Once N_i is determined, the exponential decay rate α is found from the parameter $\alpha N_i^{-1/2}$ deduced from the temperature dependence of a half-filled band. For the data of Fig. 2 we find $\alpha^{-1} = 5.26$ nm.

The values of the parameters α, W, g_0, and N_i deduced from the fit to the low-temperature data are of the order expected. The parameter α^{-1} typically has a value ranging from $3.5 < \alpha^{-1} < 7.5$ nm depending on the substrate bias, impurity concentration, and sample, and is approxi-

mately the asymptotic exponential decay rate (4.2 nm) of a 2D hydrogenic wave function corresponding to a Coulombic impurity potential on the edge of an infinite half-space.[15] The band-width W may range from 1.5 to 12.0 meV depending on the substrate bias, sodium concentration, and sample, and is less than the Coulomb scatter of the energy levels $e^2N_i^{1/2}/\kappa \sim 10$ meV, where $\kappa=7.7$ is the average permittivity at the interface. The site density N_i is found to be consistently less than surface concentration, N_{ox}, deduced from the transconductance at 77 K, but comparable to the concentration deduced from Shubnikov–de Haas measurements at 4 K. Empirically, we find that $N_i=N_{ox}/(2.40\pm0.35)$ independent of the sample, the substrate bias, and the temperature. The parameter g_0 may range from 20 to 550 mS depending on the substrate bias, the sodium concentration, and the sample, and is sensitive to errors in the estimate of W and $\alpha N_i^{-1/2}$. If we assume on the basis of a dimensional argument[4] that $g_0 \simeq e^2\omega/kT$ and determine a value for the characteristic hopping rate ω, we find that $\omega \sim 10^{13}$ sec^{-1} at 4 K, which is the correct order of magnitude.[11]

In the analysis of the temperature dependence of the conductivity of a half-filled band, we assume that the site energies are uniformly distributed over a finite bandwidth W, and that α is independent of energy in accordance with the HB model. To evaluate the energy dependence, we examined the conductivity as a function of filling fraction over the range $0<f<1$ by changing the carrier density using the gate electrode. According to the model [see Eq. (8)], a change in the energy is directly proportional to a change in carrier density at $T=0$.

In Fig. 1 the carrier dependence of the conductivity is compared with the predictions of the HB model. The solid lines in Fig. 1(a) show the results obtained from one sample by fitting the carrier density dependence as a function of N_{ox} at a constant temperature and substrate bias using the parameter N_i. In this case we find that $N_i=N_{ox}/(2.75\pm0.35)$. Figure 1(b) shows the results obtained on the same sample as a function of substrate bias at fixed temperature and impurity concentration, while Fig. 1(c) shows the corresponding results obtained at fixed impurity concentration and substrate bias as a function of temperature with $N_i=N_{ox}/2.7$. Generally, the model accurately represents the carrier density dependence of the conductivity for $\xi_c > W'$ except at low temperature [see Fig. 1(c): $T=588$ mK, $f\neq0.5$] and for $f<0.1$ and $f>0.9$.

In Figs. 5(a) and 5(b) the temperature dependence observed at four different filling factors $f=0.69$, 0.50, 0.33, and 0.08 for $V_s=0.50$ V are shown. The data at $f=0.5$ are fitted by varying three parameters. The predictions of the HB model based on these three parameters and a site density of $N_i=7.5\times10^{11}$ cm$^{-2}/2.7$ for $f=0.67$, 0.33, and 0.08 are represented by the solid lines. The temperature dependence of the chemical potential is calculated according to Eq. (8). The deviation of the fit from the data observed at low temperature for $f\neq0.5$ occurs when the condition $\xi_c < J'$ is satisfied and is generally observed for each substrate bias and sodium concentration. The deviations observed in Fig. 1(c) and in Figs. 5(a) and 5(b) occur because the average of the density of states over the energy interval $|\varepsilon_i-\tilde{\mu}|<\xi_c kT$, which determines the exponent of the conductivity, is not actually constant as a function of the filling fraction as assumed in the HB model. We conclude that the energy distribution $\rho(\varepsilon_i)$ assumed in Eq. (1) is unrealistic for filling fraction $f\neq0.5$ at low temperature and that the density of states decreases monotonically away from the center of the band. Since W has a value which is comparable to the binding energy, we do not expect either the ρ or α to be constant independent of energy over the bandwidth. The negative curvatures of the conductivity on a $T^{-1/3}$ temperature scale are consistent with a negative second derivative of the density of states with respect to energy. However, as shown in Figs. 1 and 5, the dependence of the high-temperature ($30>T>6$ K) conductivity on filling fraction is consistent with the HB model.[16] For $T>W/k\xi_c$ the conductivity is not sensitive to variations in the density of states and the approximation represented by Eq. (1) is adequate.

By changing the sodium concentration and substrate bias, the theory can be evaluated for a variety of different values of the parameters ρ, α, and g_0. For example, if we change the sodium concentration at a constant value of substrate bias, then the parameter α should not change since the structure of the wave function is, by hypothesis, the same as for an isolated impurity independent of the sodium concentration (because we assume that the overlap is small), but the density of states changes because $\rho=N_i/W$. However, if we apply a reverse (negative) substrate bias at a fixed sodium concentration, the exponential decay rate of the wave function should increase because the binding energy increases,[1] while the site density is constant. The binding energy increases because the potential at the interface due to the depletion charge forces the inversion layer closer to the sodium impurities in the oxide.

Figures 3(a) and 3(b) show the temperature dependence for a half-filled band observed at seven different sodium concentrations at a substrate bias of $V_s=0.0$ V for the same sample as in Fig. 1; the solid lines in the figure represent the results of a fit to the data in which all three parameters $\alpha N_i^{-1/2}$, W, and g_0 are permitted to vary. Figures 4(a) and 4(b) show the fit to the temperature dependence as a function of substrate bias at a sodium concentration of 7.5×10^{11} cm^{-2}. The HB model can accommodate the data for a variety of impurity concentrations and substrate-bias conditions. Figure 7 summarizes the dependence of the parameters α, W, and g_0 on impurity concentration and substrate bias for two samples ($N_i=N_{ox}/2.75$ and $N_{ox}/2.25$, respectively). The experimental error associated with the determination of the various parameters corresponds to the width of one standard deviation. We observe that the magnitude of the parameters and the trends are independent of the sample. As indicated by Fig. 7, the data taken at constant substrate bias on a number of samples are consistent with α relatively independent of sodium concentration. The value of α^{-1} typically varies less than 10% from the average over the range of N_{ox}. At a fixed substrate bias, we find that the density of states decreases as the sodium concentration decreases, but that the bandwidth W must also increase as the sodium concentration decreases to ac-

commodate the data. The bandwidth deduced from the temperature dependence increases with decreasing concentration for all of the substrate-bias conditions examined in the experiment. From data taken on a number of samples, we deduce that α increases with reverse substrate bias although it is relatively independent of sodium concentration, and that the change induced experimentally by applying a reverse substrate bias can be accommodated by the HB model provided the bandwidth increases with reverse substrate bias. The bandwidth increases with reverse substrate bias for all of the impurity concentrations examined in this work. The dependence of g_0 on the sodium concentration and substrate bias is shown at the bottom of Figs. 7(a) and 7(b). The parameter g_0 is not well defined by the fit because a 10% change in both of the parameters α and W represents a 50% change in g_0. The error in the determination of g_0 is comparable to its value.

The trends found in the bandwidth as a function of sodium concentration, substrate bias, and carrier concentration were first deduced by Fowler and Hartstein,[1] and

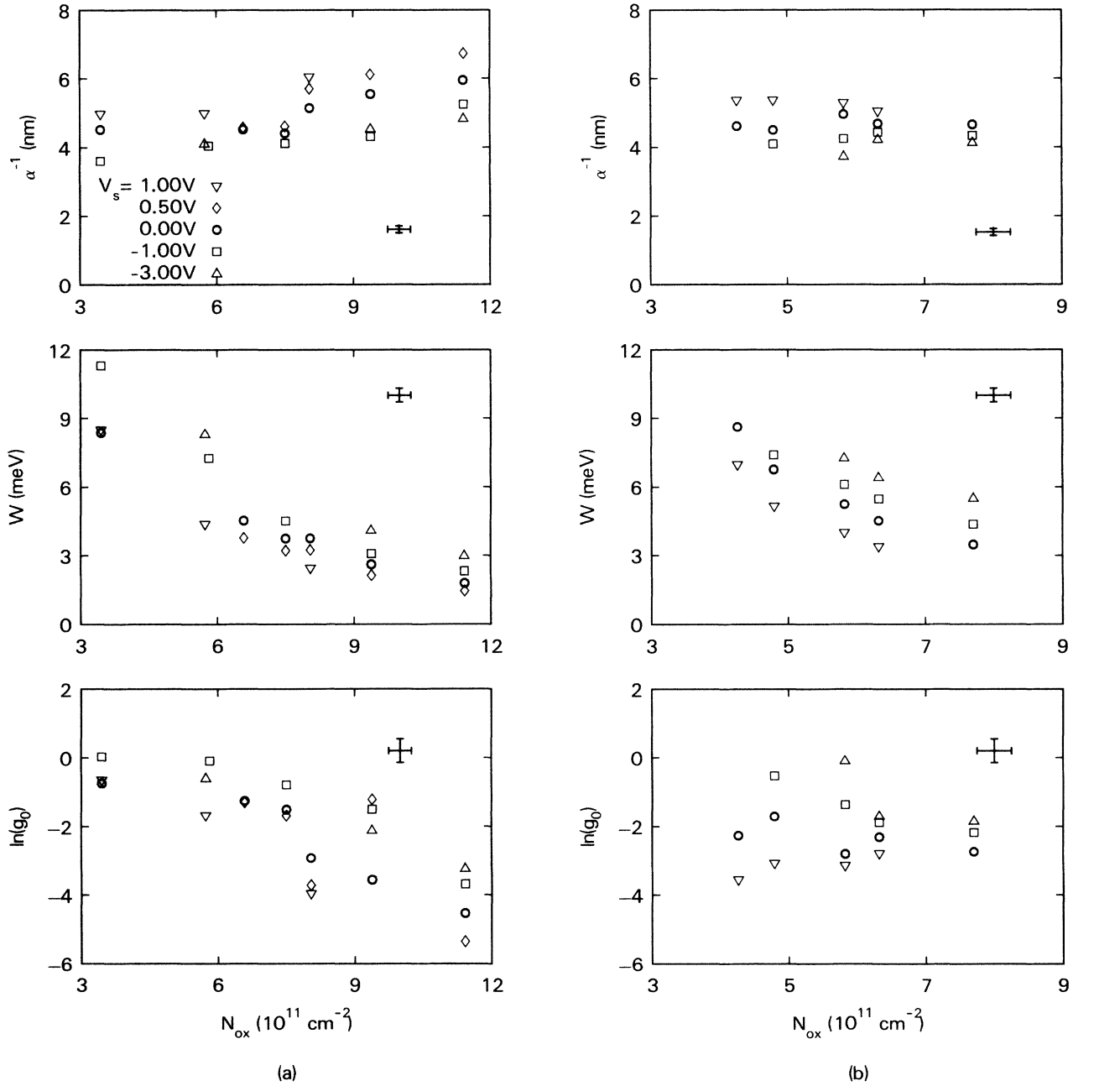

FIG. 7. Variation of the fitting parameters α^{-1}, W, and g_0 with substrate bias and sodium concentration for two different samples (a) and (b). From top to bottom: The localization length α^{-1} is plotted as a function of sodium concentration N_{ox} and substrate bias V_s; the impurity bandwidth W is plotted as a function of N_{ox} and V_s; and the logarithm of the prefactor $g_0/1$ mS is plotted as a function of N_{ox} and V_s.

Hayden[16] from the activation energies which characterize the high-temperature transport. We observe that the bandwidth increases as the wave function is compressed (i.e., as α^{-1} decreases) or as the average distance between impurities, $N_i^{-1/2}$, increases, but that the bandwidth is approximately independent of filling fraction. Figure 8(a) summarizes these observations on one sample. Figure 8(a) shows the dependence of W on the product $\alpha N_i^{-1/2}$, which is a measure of the spatial extent of the wave function relative to the intersite separation. Although the product $\alpha N_i^{-1/2}$ is varied by changing α and N_i independently by the varying substrate bias and the surface impurity concentration, respectively, we find that the bandwidth increases as the overlap between neighboring impurity sites decreases independent of how the overlap is varied. As shown in Fig. 8(b) the same trend is observed in different samples.

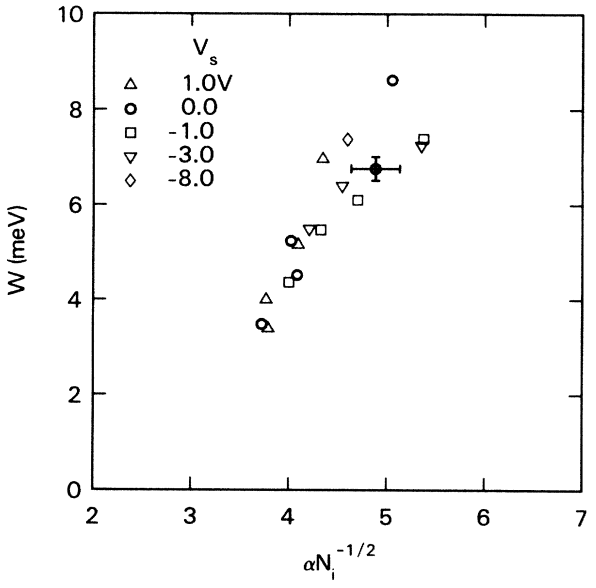

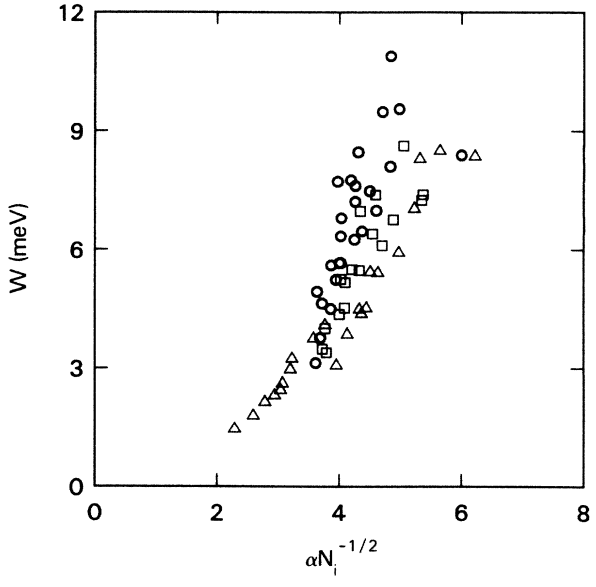

FIG. 8. In (a) the impurity bandwidth W is plotted vs $\alpha N_i^{-1/2}$ with substrate bias and sodium concentration as parameters. In (b) the impurity bandwidth is plotted vs $\alpha N_i^{-1/2}$ with the sample as the parameter. The three different symbols (square, circle, and triangle) represent three different samples.

The trend observed in the bandwidth W is not understood. It is implicitly assumed in the HB model that the contribution to the site energy (and therefore the bandwidth) arising from the overlap of wave functions corresponding to different centers is negligible, and the data are consistent with this assumption. The bandwidth $\Delta\varepsilon$ associated with the overlap between neighboring sites is approximately equal to the product of the binding energy and the overlap integral,[10,17]

$$\Delta\varepsilon = E_c e^{-\alpha N_i^{-1/2}}, \tag{12}$$

which varies from 10 μeV to 1.5 meV for $3\times10^{11} < N_{ox} < 1.1\times10^{12}$ cm^{-2}, while the bandwidth deduced from the fit to the temperature dependence using the HB model varies from 1.7 to 12 meV over the same range of concentration. Thus, the contribution to the site energy arising from the overlap which is an exponentially increasing function of impurity concentration is negligible, except at the highest concentration.

Pollak[18] interpreted the observed increase in the activation energy with decreasing N_{ox} by appealing to multielectron hopping which arises through electron-electron interactions. According to Pollak, another associated effect would be a decrease of the temperature independent factor in the high-temperature conductivity $\sigma(T=\infty)$ from the noninteracting value, which would become more pronounced with increasing N_{ox}. Although we observe an increase in the activation energy, we find that the change observed in $\sigma(T=\infty)$ with N_{ox} can be accommodated by the noninteracting (HB) model with α and g_0 varying as shown in Fig. 7. A thorough comparison of the data with multielectron hopping theory is frustrated by the present lack of a quantitative model for correlated transport in two dimensions.

The observed temperature dependence of the conductivity is not consistent with the temperature dependence predicted by Efros and Shklovskii[5] for a Coulomb gap in the single-particle excitation spectrum. The effect of the intersite Coulomb repulsion between electrons $\Delta\sim e^2 N_i^{1/2}/\kappa$ was ignored in analysis of the data given above, but the gap in the single-particle excitation spectrum which results from the Coulomb interaction is estimated[6] to be $\Delta\sqrt{\Delta/W}\sim10$ meV. It is not appropriate to ignore the Coulomb interaction if it is comparable to the disorder energy W or the thermal energy. Efros and Shklovskii[5] have shown that the single-particle density of states vanishes at the Fermi level according to $\rho(\varepsilon)=\kappa^2|\varepsilon|/e^4$ in two dimensions because of the intersite Coulomb repulsion.[19] The depletion of the low-energy excitations by the Coulomb interaction impedes variable-range hopping for

$$T < T_c = \frac{e^4}{\kappa\alpha}\frac{N_i}{W}$$

and causes the conductivity to be activated. At low temperature ($T \ll T_c$) the conductivity is characterized by the law

$$\sigma = \sigma_0 \exp[-(T_0/T)^{1/2}] ,$$

where the temperature $T_0 = 6.2e^2\alpha/\kappa$.

To investigate the effect of the intersite Coulomb repulsion, we examined the temperature dependence to determine if the low-temperature conductivity could be fitted to the law $\sigma \sim \exp[-(T_0/T)^{1/2}]$ proposed by Efros and Shklovskii.[5] The deviation of a $T^{-1/2}$ law from the data over a temperature regime in which the optimum exponent is one-half is represented by the line in the lower portion of Fig. 2. Although we can generally fit the low-temperature data for a half-filled band to this functional dependence over a limited temperature regime, under conditions in which the sensitivity and the temperature range accessible in these experiments are optimized, the conductivity is consistently found to deviate from a $T^{-1/2}$ law at low temperatuare toward a $T^{-1/3}$ law. In the regime in which the conductivity can be described by a $T^{-1/2}$ law we find that T_0 varies between $100 < T_0 < 550$ K depending on the substrate bias and sodium concentration. The localization length deduced from T_0 is found to range from $42.3 > \alpha^{-1} > 22.1$ nm, which is approximately an order of magnitude larger than the corresponding value for a 2D Coulomb potential. Although the temperature dependence of the conductivity corresponding to a Coulomb gap in the single-particle excitation spectrum can be fitted to the data over a limited range, the data are not generally consistent with a $T^{-1/2}$ law at low temperature, and the exponential decay rate necessary to fit the data is unrealistically small, so that the conductivity observed at low temperature is larger than that predicted by the interacting model.

B. Non-Ohmic conduction

The non-Ohmic conductivity is consistent with the model for hopping in moderate fields proposed by Shklovskii.[7] In Fig. 6 a typical plot of the logarithm of the channel current versus $F^{0.429}$ and F, for $f = 0.5$ in a temperature regime in which the Ohmic conductivity is given by the condition $\xi_c < K'$, is compared with a fit to a form suggested by Shklovskii's theory for non-Ohmic hopping conduction: $i = i_0 \exp(F/F)^{0.429}$. We find the prediction of electric field dependence obtained from the non-Ohmic, interacting percolation model describes the field dependence of the current over the range where the theory applies. The best fit to the low-temperature data is generally given by $i = i_0 \exp(F/F_0)^x$, where $0.38 < x < 0.52$ for electric fields $F < 150$ V/cm. In the lower portion of the figure, the deviation of the fit from the data is shown. The deviation from the fit observed at high fields may be associated with a nonuniform density of states across the channel (the drain-source voltage was 10% of the gate voltage), while the deviation found at low fields is indicative of a transition to Ohmic behavior. Our results are not consistent with the field dependence predicted by Pollak and Riess[20] to occur in the same range of electric field for a two-dimensional system. A plot of the logarithm of the non-Ohmic current versus F is shown in Fig. 6. The data are not well represented by the law $i = i_0 \exp(F/F_0)$ predicted by Pollak and Riess to apply for $F < 2kT\alpha/e$.

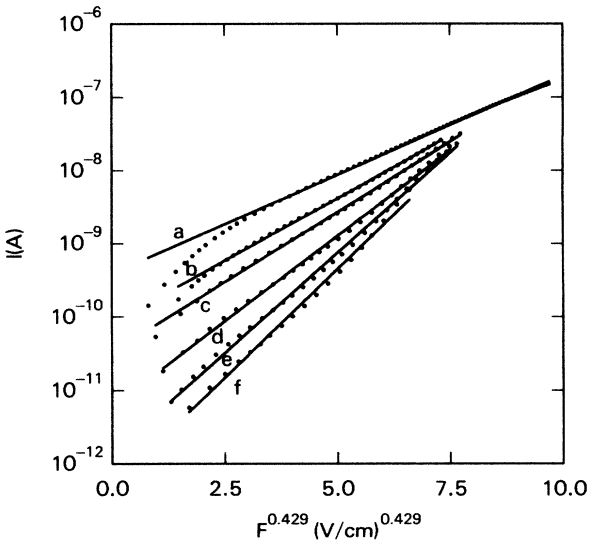

FIG. 9. Current-electric field characteristic as a function of temperature for a half-filled band with $N_{ox} = 5.2 \times 10^{11}$ cm^{-2} ($N_i = 2.6 \times 10^{11}$ cm^{-2}) and $V_s = 0$ V. The solid lines in the figure represent fits to Shklovskii's theory for non-Ohmic conduction. In the figure the temperatures and fitting parameters are, respectively, a, $T = 4.22$ K and $F_0 = 1.94$ V/cm; b, 3.22 K and 1.75 V/cm; c, 2.76 K and 1.36 V/cm; d, 2.16 K and 1.01 V/cm; e, 1.84 K and 0.745 V/cm; and f, 1.58 K and 0.500 V/cm.

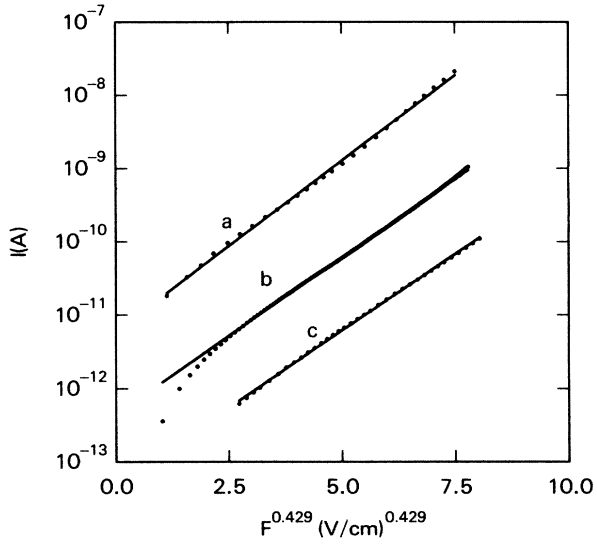

FIG. 10. Dependence of the current-electric field characteristic on impurity concentration for a half-filled with $V_s = 0$ V and T = 2.17 K. ($N_i = N_{ox}/2.0$.) The solid lines in the figure represent fits to Shklovskii's theory for non-Ohmic conduction. In the figure the impurity concentrations and fitting parameters are, respectively, a, $N_{ox} = 5.6 \times 10^{11}$ cm^{-2} and $F_0 = 1.01$ V/cm; b, 4.6×10^{11} cm^{-2} and 1.03 V/cm; and c, 4.0×10^{11} cm^{-2} and 0.888 V/cm.

The dependence of the fitting parameter F_0 is also consistent with the prediction given by Eq. (11). Figures 9, 10, and 11 show the temperature, impurity concentration, and substrate-bias dependences of the current-field characteristic, respectively. The slope increases with decreasing temperature but is relatively insensitive to impurity concentration and substrate bias over the range examined in these experiments. In Fig. 12 the electric field F_0 deduced from the fit to the current-field characteristic under a variety of conditions in one sample is compared with F_0 calculated from the measured temperature and the parameters, α and ρ, deduced from the Ohmic temperature dependence. We find that if the constant $C=0.32$ in Eq. (11), then the measured slope is consistent with the predictions of the model.

V. SUMMARY

We have shown that the temperature and electric field dependence of hopping conduction observed in a half-filled, strongly localized 2D impurity band are consistent with noninteracting single-particle models based on percolation theory. The Ohmic conductivity at low temperature follows the law for variable range hopping in 2D, $\sigma \sim \exp[-(T_0/T)^{1/3}]$, while at high temperature the transport is activated with an activation energy proportional to the bandwidth. The localization length α^{-1} deduced from the fit to the temperature dependence is observed to be relatively independent of impurity concentration but decreases with increasing surface electric field.

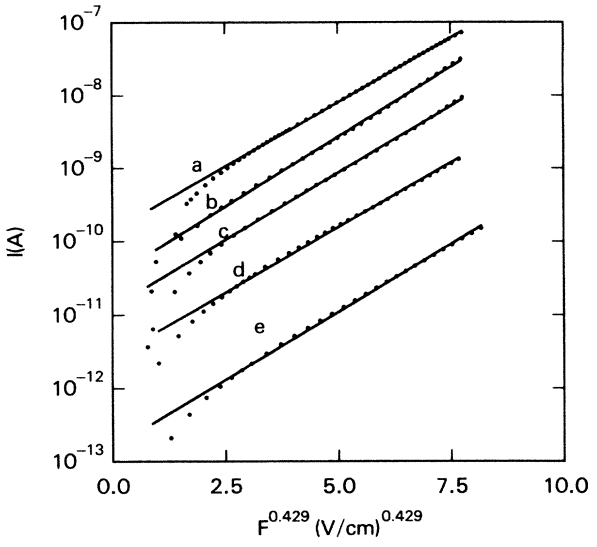

FIG. 11. Dependence of the current-electric field characteristic on substrates bias for a half-filled band with $N_{ox}=5.2\times10^{11}$ cm^{-2} ($N_i=2.6\times10^{11}$ cm^{-2}) and $T=2.78$ K. The solid lines in the figure represent the fits to Shklovskii's theory for non-Ohmic conduction. In the figure the substrate bias conditions and fitting parameters are, respectively, a, $V_s=0.5$ V and $F_0=1.56$ V/cm; b, 0.0 V and 1.35 V/cm; c, -1.0 V and 1.45 V/cm; d, -3.0 V and 1.64 V/cm; and e, -8.0 V and 1.58 V/cm.

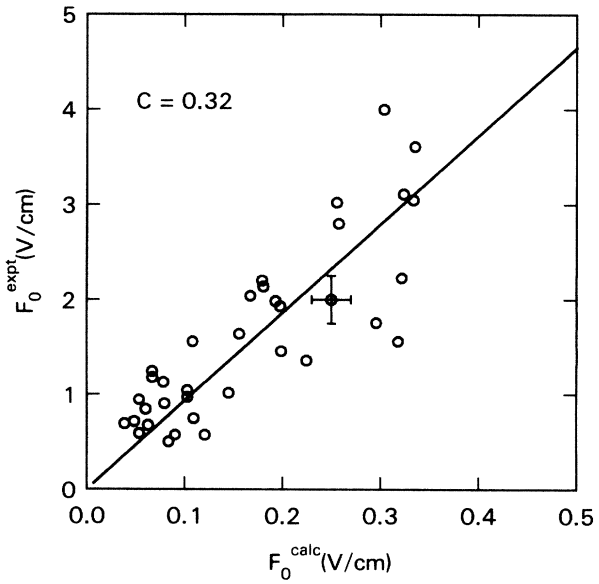

FIG. 12. Comparison of the field F_0^{exp} which characterizes the non-Ohmic current observed for a half-filled impurity band and F_0^{cal} determined according to Eq. (11) in the text. The solid line in the figure represents a fit to the data assuming $C=0.32$.

The bandwidth W is found to increase with reverse substrate bias and decreasing impurity concentration. The predictions of the HB model are not generally consistent with the low-temperature conductivity for $f\neq0.5$ because the approximations that the density of states is uniform and α is independent of energy are not valid. The temperature dependence of the Ohmic conductivity is not generally consistent with the temperature dependence predicted by Efros and Shklovskii[5] for a Coulomb gap in the excitation spectrum, although the gap was expected to determine the conductivity under the conditions examined in these experiments. The failure of the interacting model proposed by Efros and Shklovskii to describe the data does not preclude the existence of carrier-carrier interactions, however. In particular, Mott[21] has predicted $\sigma \sim \exp[-(T_0/T)^{1/3}]$ behavior at low temperature based on an interacting, multielectron hopping model.

We observe that the current-field characteristic is non-Ohmic for fields $5<F<150$ V/cm, and the logarithm of the current is observed to be linearly related to $F^{0.429}$. The current-field characteristic and the slope of the logarithm of the current versus $F^{0.429}$ was found to be consistent with the predictions of a model for non-Ohmic conduction in 2D proposed by Shklovskii.[7] The electric field dependence of the non-Ohmic current is not consistent with the model proposed by Pollak and Riess.[20]

ACKNOWLEDGMENT

The authors gratefully acknowledge several useful discussions of the data with M. Pollak, F. Stern, J. Davies, and H. Reisinger and wish to thank H. Euler, H. Harris, and J. Tornello for their technical assistance.

[1]A. B. Fowler and A. Hartstein, Philos. Mag. B **42**, 949 (1980).
[2]T. Ando, F. Stern, and A. B. Fowler, Rev. Mod. Phys. **54**, 437 (1982).
[3]P. W. Anderson, Phys. Rev. **109**, 1492 (1958).
[4]K. T. Hayden and P. N. Butcher, Philos. Mag. B **38**, 603 (1979).
[5]A. L. Efros and B. I. Shklovskii, J. Phys. C **8**, L49 (1975).
[6]M. Pollak, Discuss. Faraday Soc. **50**, 13 (1970); M. Pollak and M. L. Knotek, J. Non-Cryst. Solids **32**, 141 (1979).
[7]B. I. Shklovskii, Fiz. Tekh. Poluprovidn. **10**, 1440 (1976) [Sov. Phys.—Semicond. **10**, 855 (1976)].
[8]N. F. Mott, M. Pepper, S. Pollitt, R. H. Wallis, and C. J. Adkins, Proc. R. Soc. London, Ser. A **345**, 169 (1975); M. Pepper, S. Pollitt, and C. J. Adkins, J. Phys. C **7**, L273 (1974).
[9]D. J. DiMaria, J. Appl. Phys. **48**, 5149 (1978).
[10]V. Ambegaokor, B. I. Halperin, and J. S. Langer, Phys. Rev. B **4**, 2612 (1971).
[11]A. Miller and E. Abrahams, Phys. Rev. **120**, 745 (1960).
[12]C. H. Seager and G. E. Pike, Phys. Rev. B **10**, 1435 (1974).
[13]M. E Levinshtein, B. I. Shklovskii, M. S. Shur, and A. L. Efors, Zh. Eksp. Teor. Fiz. **69**, 386 (1975) [Sov. Phys.—JETP **42**, 197 (1976)].
[14]R. Fletcher and M. J. D. Powell, Comput. J. **6**, 163 (1963).
[15]Ch. Zeller and G. Timp (unpublished); and N. O. Lipari, J. Vac. Sci. Technol. **15**, 1412 (1978).
[16]K. J. Hayden, Philos. Mag. B **41**, 619 (1980).
[17]B. I. Shklovskii and A. L. Efros, *Electronic Properties of Doped Semiconductors* (Springer-Verlag, New York, 1984).
[18]M. Pollak, Surf. Sci. **113**, 170 (1982).
[19]The proximity of the metal gate transforms the Coulomb repulsion into a dipole interaction for $r_{ij} > d$, where d represents the thickness of the oxide. Consequently, the density of states at the Fermi level is finite and is of the order $\rho = \kappa d^2 / e^2 \alpha$.
[20]M. Pollak and I. Riess, J. Phys. C **9**, 2339 (1976).
[21]N. F. Mott, Philos. Mag. **34**, 643 (1976).